Journal Name

ARTICLE

Formation of Resorcinol-Formaldehyde Hollow Nanoshells through a Dissolution-Regrowth Process

Received 00th January 20xx,
Accepted 00th January 20xx

DOI: 10.1039/x0xx00000x

www.rsc.org/

Shuai Zhou,[a,b] Yaocai Bai,[a] Wenjing Xu,[a] Ji Feng,[a] Xiaojing Wang,[a] Zhiwei Li,[a] Yadong Yin[a]*

We report here that dissolution and regrowth of resorcinol formaldehyde (RF) colloidal particles can occur spontaneously when they are subjected to etching in solvents such as ethanol and tetrahydrofuran, resulting in the formation of hollow nanostructures with controllable shell thickness. The hollowing process of the RF particles is attributed to their structural inhomogeneity, which is resulting from the successive deposition of oligomers with different chain lengths during their initial growth. As the near-surface layer of RF colloids mainly consists of long-chain oligomers while the inner part of short-chain oligomers, selective etching removes the latter and produces the hollow structures. By revealing the important effects of the condensation degree of RF, the etching time and temperature, and the composition of solvents, we demonstrate that the morphology and structure of the resulting RF nanostructures can be conveniently and precisely controlled. This study not only improves our understanding of the structural heterogeneity of colloidal polymer particles, but also provides a practical and universal self-templated approach for the synthesis of hollow nanostructures.

Introduction

Nanostructured polymers, especially phenolic resin-based materials have won wide recognition in the fields of drug release, gene delivery and bioimaging due to their remarkable biocompatibility for biomedical applications.[1-4] Furthermore, nanostructured phenolic resins have been widely used in the synthesis of various nanostructured carbon materials, presenting great value as catalysts, adsorbents, supercapacitors, lithium-ion battery electrodes and drug delivery carriers.[5-17] Synthesis of phenolic resin nanospheres with precisely controlled sizes has been widely studied.[18-20] In a typical synthesis, the polymerization of resorcinol and formaldehyde is achieved via a modified Stöber method, using ammonia solutions as catalysts.[21] However, most of the works neglect the study of product compositions, which are highly important to understand the polymerization process and provide more opportunities for the design and synthesis of complicated nanostructures.[20-22] Considering that the phenolic resin is endowed with a typical crosslinking structure, and that the reaction proceeds with a continuous increase in the crosslinking degree, then, the polymerization degree of inner and outer parts of the RF colloids may be different. Therefore, one could selectively etch the low polymerized areas by solvents to obtain hollow nanostructures.[23, 24] Taking advantage of the structural difference, Wan and co-authors used acetone to selectively remove the interior part of the 3-aminophenol/formaldehyde resin to obtain hollow nanospheres[25].

We report here the development of a spontaneous dissolution-regrowth process for the self-templated synthesis of hollow RF nanostructures with controllable shell thicknesses. The key finding is the structural heterogeneity in the RF colloidal particles formed during their synthesis by the Stöber-like method, where the near-surface and interior regions are composed of polymer chains of different lengths. Hollow nanostructures can be produced by selectively etching the interior, which consists of short-chain oligomers, while retaining the more robust near-surface layer composed of oligomers with relatively longer chains. We reveal that the formation of the hollow structure is affected by the reaction time, temperature, and composition of solvents used in both the initial RF synthesis and the etching process, which, in combination with the regrowth of the shells by redeposition of the dissolved oligomers, offer great opportunities to conveniently and precisely control the morphology of the polymer nanoshells.

Results and discussion

Briefly, the RF resin colloids were prepared via a modified Stöber method, and the specific preparation details were shown in the Supporting Information.[21] According to the reaction mechanism of phenolic resin colloids, higher reaction temperature and longer reaction favour the condensation of RF resin colloids. Therefore, synthesizing RF resin colloids at room temperature (RT) for relatively short reaction time allows us to better study the mechanism of RF dissolution-regrowth process by means of direct solvent etching. As shown in Figure 1a, the RF resin colloids prepared in an aqueous

[a] Department of Chemistry, University of California, Riverside, California 92521, USA. E-mail: yadong.yin@ucr.edu
[b] College of Science, Nanjing Forestry University, Nanjing 210037, China
[c] † Electronic Supplementary Information (ESI) available: Experimental section. See DOI: 10.1039/x0xx00000x

solution at RT for 1 h are well-dispersed. It could be observed in Figure 1b that, after etching the as-prepared RF colloids with ethanol for 10 min, the inner part of the RF resin colloids could be removed. Even though there was a lack of support inside the RF resin colloids, the hollow RF shells maintained a regular spherical structure. The preparation is reproducible and easily scalable to produce a large amount of hollow RF shells with a high yield (Figure S3a). Interestingly, when the etching time was extended to 360 min, the shell thickness increased, as displayed in Figure 1c. In order to better characterize the structural change by time, the inside and outside diameters of RF hollow nanoshells were measured. The shell thickness was calculated accordingly, and plotted versus the etching time, as shown in Figure 1d. When the etching time was prolonged, the shell thickness gradually increased from 41 nm to 71 nm. Meanwhile, the outside diameters of RF resin colloids witnessed an increase from 472 nm to 495 nm and the inside diameters of hollow RF colloids decreased from 390 nm to 353 nm, further confirming that the dissolved RF oligomer chains from the internal part can regrow on both sides of RF colloids nanoshell. Because the particles were cleaned before etching, we believe that the RF oligomer chains dissolved from the core area can regrow on both sides of the RF nanoshells. In addition, shorter etching was performed in order to better track the dissolution and regrowth processes. Monitoring the morphology of RF hollow nanoparticles after etching in ethanol for 1 min and 2.5 min clearly indicates that the etching started from the inside of RF resin colloids (Figure S1). When the etching time was extended to 2.5 min, robust nanoshells were obtained, with a small increase in the shell thickness than the 1-min sample, suggesting that although dissolution and regrowth processes took place simultaneously, the rate of dissolution was much higher than that of the RF regrowth at the early stage of the reaction. It should be noted that there was a small residual core structure inside the RF hollow nanoparticle, regardless of the length of etching time. The possible mechanism will be discussed later. The optical transmittance of the colloidal dispersions was monitored to assist our understanding of the etching and regrowth process. As displayed in Figure 1e, the transmittance was the lowest in the initial RF colloids (~10%). It increased sharply to 72% after etching for 5 min, suggesting again rapid etching at the early stage of the reaction. Subsequently, the transmittance decreased gradually and reached 21% at 360 min, indicating more dominant growth than etching.

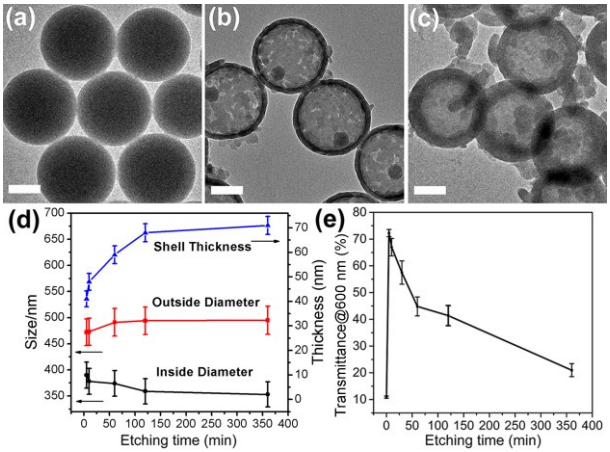

Figure 1. TEM images of RF resin colloids prepared at RT for 1 h (a), and hollow RF nanostructures prepared by 1 mL of ethanol etching at RT for (b) 10 min, and (c) 360 min. Scale bars = 200 nm. (d) The size changes of the outside diameter, the inside diameter, and the shell thickness of RF nanoshells for different ethanol etching time. All samples were treated with 1 mL of ethanol at RT. (e) The transmittance of RF resin colloids with 1 mL of ethanol etching at RT for 5 min, 10 min, 60 min, 120 min, 360 min, and the transmittance at 0 min corresponding to the RF resin colloids dispersed in water before ethanol etching. Note that the transmittance was recorded at 600 nm.

The hollowing strategy is developed based on our understanding that the inner and outer parts of RF colloids are of different polymerization degrees, and that the limited solubility in ethanol leads to the preferred dissolution of oligomers with a shorter chain length.[26] In order to verify the heterogeneity within the RF resin colloids, tetrahydrofuran (THF) was used to dissolve the remaining nanoshells that were produced by ethanol etching, since THF has a significantly higher solubility than ethanol toward RF resins.[27] Matrix-Assisted Laser Desorption/Ionization-Time Of Flight (MALDI-TOF) mass spectrometry (MS) was used to analyze the composition of RF released from the inner and outer parts.[28] In a typical experiment, the supernatant from the ethanol etching step was separated from the residual RF nanoshells, which were then completely dissolved in THF. Figure 2a showed the mass distribution of supernatant obtained after ethanol etching. It is obvious that the oligomers with a molecular weight below 551 dominate the products, meaning that the interior of RF resin colloids was mainly composed of oligomers of shorter chains (dimer, trimer, and tetramer). The inset image shows the molecular structure of a typical monomer structure, which corresponds to the molecular weight in mass distribution. The formation mechanism of the monomer was displayed in Figure S2. The first methylation of the amine begins with active imine formation with formaldehyde, and the active imine and resorcinol further undergo para nucleophilic additions with aminomethyl connected. The active terminal primary amine can be further condensed with formaldehyde to form an imine bond (Schiff base bond). Finally, the imine is partially hydrolyzed under basic conditions to form the proposed monomer product. As a strong solvent, THF can completely etch the residual RF nanoshells prepared at RT, resulting in a completely transparent solution.[29] As shown in Figure 2b, the oligomers with a molecular weight ranging from 536 to 900 dominate the products, and the distribution below 500 molecular weight only accounts for a small fraction, indicating that the outer nanoshell consisted of oligomers with relatively longer chains. Although the above analysis is not strictly quantitative, it is still safe to conclude that the composition of sol-gel derived RF spheres were inherently heterogeneous, with shorter chains in the core region and longer chains near the surface, allowing selective etching of the core by a relatively weak solvent such as ethanol. On the other hand, the dissolved oligomers with an increasing concentration may regrow and deposit on the shell surface as catalyzed by the ammonium ions adsorbed on the shell surface.

Although it is difficult to obtain direct evidence regarding the formation mechanism of the remaining residue core, we believe it still relates to the compositional inhomogeneity of the polymer at different stages of nucleation and growth, in a way

similar to the case of silica colloids during their formation in the Stöber process.[13, 30, 31] When resorcinol and formaldehyde react to form oligomers at the beginning of the reaction, the solubility of the products decreases as the polymerization proceeds.[23, 24] Supersaturation occurs when the oligomers reach sufficient size and concentrations, producing nuclei that are composed of primarily long-chain polymers. The nucleation consumes most of the long-chain oligomers so that the subsequent growth is driven by the deposition of short-chain oligomers to the nuclei surface.[31-33] The size of these oligomers increases over a relatively long growth period so that the near-surface layer is composed of long-chain oligomers. In the end, the colloidal RF spheres have a long-short-long sandwich structure. Upon etching, the part with shorter oligomer chains is removed first by ethanol, leaving the core and shell of longer oligomer chains. When subjected to a strong solvent such as THF, the RF spheres can be dissolved completely due to the small difference in solubility between the short and long chains.

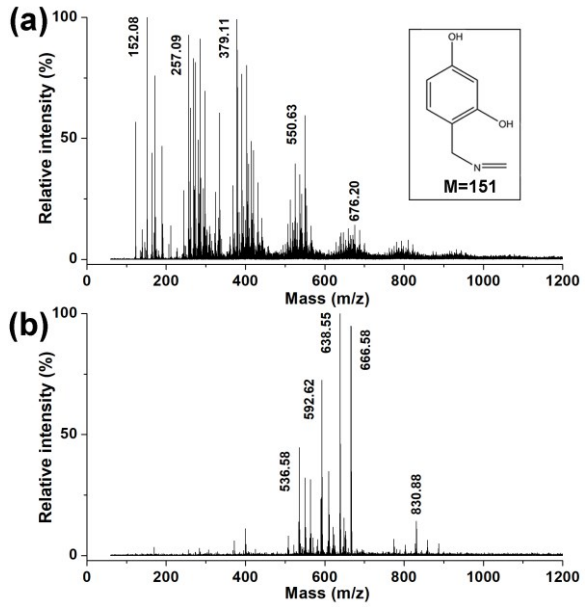

Figure 2. (a) Representative MALDI-TOF MS analysis of supernatant from ethanol etching collected by centrifuge. RF colloids prepared at RT for 1 h and etched at RT by 1 mL of ethanol. Inset: Proposed monomer molecular structure, corresponding to the mass value ($M+H^+$=152.05). (b) MALDI TOF MS analysis of solution for the residual precipitate completely etched at RT by 1 mL of THF, the residual precipitate obtained by centrifugation from ethanol etching solution.

Apart from etching time, the effect of RF condensation degree, etching temperature, and etching solvents on the morphologies and structure of the resulted RF resin colloids were also investigated in detail. The RF condensation degree can be tuned by controlling the reaction temperature and reaction time. When the polymerization temperature was increased from room temperature to 50 °C, the prepared RF colloids could not be etched by ethanol at room temperature (Figure S4a), indicating that increasing the polymerization temperature can effectively improve the condensation degree of RF. Here, we further explored the effect of reaction time on the condensation of RF. We first condensed the RF colloids at room temperature for 30 min, 2 h, and 24 h, which were then etched by ethanol. The resulting nanostructures are shown in Figures 3a-c. Compared with the robust nanoshells produced from the sample with 2-h condensation (Figure 3b), 30-min condensation only led to a very low degree of crosslinking so that the RF nanoshells obtained after etching were irregular and unstable (Figure 3a). When extending the condensation time to 24 h, as shown in Figure 3c, the RF colloids could not be etched at all even after leaving the sample in ethanol for 12 h, indicating significantly enhanced crosslinking degree and reduced solubility of the polymer. Interestingly, when the same RF spheres (with 24-h condensation) were treated in THF, soft nanoshells could be obtained (Figure 3d), suggesting more substantial condensation in the near-surface region than the interior of the spheres. Dimethylformamide (DMF), which was known as a stronger solvent than THF,[25] completely dissolved the RF spheres that were condensed for 24 h at room temperature. When the RF spheres and as-prepared nanoshells were heated in water at 100 °C for 3 h, substantial crosslinking was achieved. As a result, these highly crosslinked RF colloids and RF nanoshells could not be etched by DMF even after etching for 4.5 days, as shown in Figure 3e and Figure S3b.

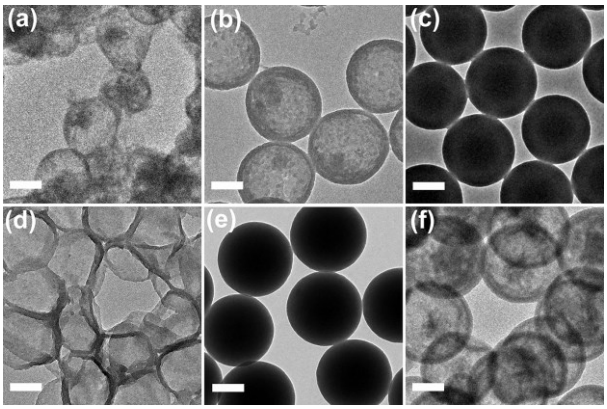

Figure 3. TEM images of RF colloids (a) prepared at RT for 30 min and then etched with 1 mL of ethanol at RT for 10 min, (b) prepared at RT for 2 h and then etched with 1 mL of ethanol at RT for 10 min, (c) prepared at RT for 24 h and then etched with 1 mL of ethanol at RT for 12 h, (d) prepared at RT for 24 h and then etched with 1 mL of THF at RT for 12 h, (e) prepared at RT for 24 h and dispersed in water at 100 °C for 3 h, and then etched with 1 mL of DMF at RT for 4.5 d, (f) prepared at RT for 30 min and then etched with 1 mL of ethanol at 60 °C for 10 min. Scale bars = 200 nm.

As expected, the structure of the nanoshells could be fine-tuned by adjusting the etching parameters such as the type of solvent and the etching time and temperature. Figure 3f showed the structure of the RF resin colloids prepared by condensing the initial RF spheres at RT for 30 min and then etching in ethanol

at 60 °C for 10 min. Compared with the very soft nanostructures produced by etching at RT in Figure 3a, the nanoshells became thicker, and the edge of the nanoshell is well-defined. The improvement of nanoshell morphology is believed to benefit from the rapid dissolution of the short-chain oligomers in the early stage of the reaction and the significant increase in their concentration at the later stage. The latter is driven by the fast solvent evaporation, thus enhancing the supersaturation of the oligomers and their more substantial deposition on the nanoshells.

This dissolution-regrowth process is highly related to the initial synthesis conditions for solid RF spheres, especially the volume ratio of ethanol/water in the preparation solution. As previously reported, the diameters of RF colloids can be widely tuned by controlling the ratio of ethanol/water in reaction solutions.[21] Besides the size control, it was found that the degree of RF condensation can be effectively regulated by adjusting the ratio of ethanol/water in RF preparation solutions.[34] As depicted in Figure 4a and Figure S5a, when the volume ratio of ethanol/water was 0 mL / 25 mL, most inner part of RF colloids could be etched by ethanol in 10 min and typical hollow nanospheres could be obtained. As the volume ratio of ethanol/water was increased to 5 mL / 20 mL, it was obvious that RF colloids could only be partially etched (Figure 4b), producing porous spheres. No apparent etching by ethanol could be observed for the volume ratio of 10 mL: 15 mL, as shown in Figure 4c. Considering the higher solubility of short-chain oligomers in ethanol than that in water, the growth of RF spheres in a solution with more ethanol is driven by the precipitation of oligomers of larger sizes. As-synthesized RF spheres, therefore, are more resistant to etching.[26]

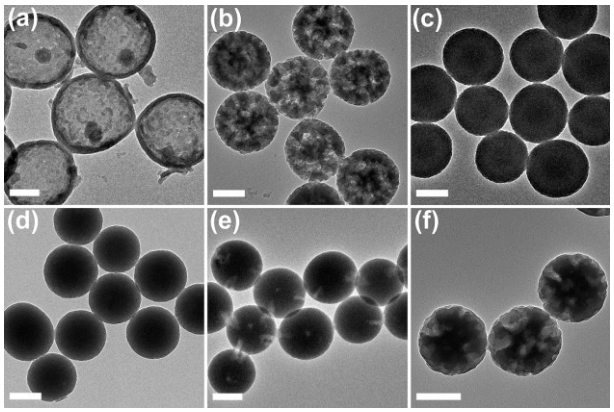

Figure 4. (a-c) TEM images of RF colloids first prepared with different volume ratios of ethanol/water: volume ratio of ethanol/water = (a) 0 mL: 25 mL, (b) 5 mL : 20 mL, (c) 10 mL : 15 mL, at RT for 1 h, and then etched with 1 mL of ethanol at RT for 10 min. (d-f) TEM images of RF colloids prepared with a volume ratio of ethanol/water: 5 mL: 20 mL at RT for 1 h, and then etched with 2 mL of ethanol and water mixture with a different volume ratio of ethanol/water: volume ratio of ethanol/water = (d) 1:4, (e) 1:2, (f) 1:1 at RT for 10 min. Scale bars = 200 nm.

In addition, it was confirmed that the amount of NH_4OH and the formaldehyde/resorcinol (F/R) ratio had a significant effect on the condensation degree of RF colloids. When the NH_4OH volume was increased to 420 μL (three times the volume of ammonia in the standard preparation process), the as-prepared RF colloids could not be partially etched by 1 mL of ethanol (Figure S4b), indicating that increasing the concentration of ammonia can enhance the condensation of RF colloids. To further investigate the effect of F/R ratio on the etching process, the F/R ratio was decreased from the standard 70 μL: 50 mg to 17.5 μL: 50 mg. As shown in Figure S4c, most of the RF colloids were etched by 1 mL of ethanol and the dissolved oligomers were further re-polymerized to form an irregular and aggregated structure. A smaller F/R ratio likely resulted in a lower crosslinking degree of the RF colloids, leading to their easy dissolution in ethanol.

Moreover, the dissolution-regrowth of RF is influenced by the composition of the etching solvent. We first prepared RF spheres with ethanol/water at the volume ratio of 5 mL: 20 mL, and collected them from a 2-mL for etching. To maintain the same RF concentration during preparation and etching, 2 mL of etching solution with different composition was added to each sample. It should be noted that in all previous etching processes 1 mL of solvent was used. As shown in Figure 4d and Figure S5b, when the volume ratio of ethanol/water in the etching solution was 1:4, RF resin colloids kept its original solid spheres structure, meaning that RF resin colloids cannot be etched when the volume ratio of ethanol/water in the etching solution was the same as that in the RF preparation solution. When the volume ratio of ethanol/water of etching solution was increased to 1:2, only a small part of RF resin colloids started to be etched, as displayed in Figure 4e. When continuing to raise the ratio of etching solution to 1: 1, it was found in Figure 4f and Figure S5c that the etching degree of RF resin colloids was significantly increased, and typical porous nanospheres can be readily obtained. Relying on the above information, a reasonable conclusion can be drawn that RF resin colloids can also be selectively etched when the volume ratio of ethanol/water in the etching solution is higher than that in the RF preparation solution.

This dissolution-regrowth method could prepare the hollow sphere not only from pure RF resin spheres but also from RF coated nanostructures. For example, when the prepared RF resin colloids were re-coated with RF, and then subject to ethanol etching, monodisperse yolk-shell RF@RF nanostructures were constructed (Figure 5a and Figure S6a). When Fe_3O_4 nanospheres were coated with RF, yolk-shell Fe_3O_4@RF nanospheres (Figure 5b and Figure S6b) were synthesized by the following ethanol etching.[35, 36] The magnetic core may allow convenient assembly into nanochain structures.[37] Figure 5c and Figure S6c showed that after coating with RF, the core-shell FeOOH@RF nanostructures can be converted into yolk-shell structures by ethanol etching. Because FeOOH nanorods are the main source for the preparation of magnetic nanorods, such nonspherical structures may be useful in nanoscale magnetic material preparation and nanoscale

magnetic control.[38] Noble metal nanoparticles such as silver were coated with a layer of RF and then transformed into yolk-shell structures with silver particles inside hollow RF nanoshells (Figure 5d and Figure S6d),[39] which may find potential applications in catalysis.[39] High scalability in producing these yolk-shell nanostructures improves their potential for practical applications. Furthermore, after selective etching, the permeability of the RF nanoshells improves (Figures S7a-b), allowing the further growth of silver on the surface of Au seeds that were confined in these nanostructured reactors (Figure S7c).

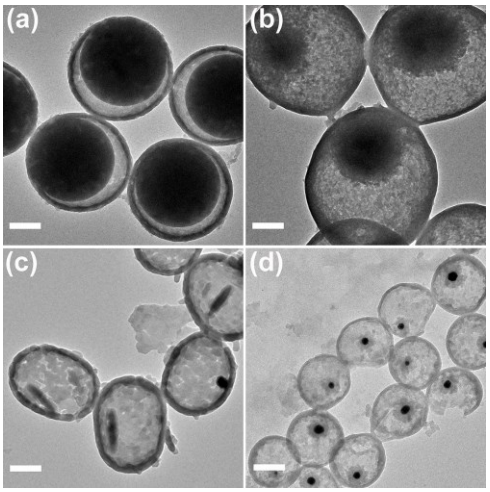

Figure 5. TEM images of yolk-shell structures produced by reacting with core-shell (a) RF@RF spheres, (b) Fe_3O_4@RF spheres, (c) FeOOH@RF spheres, (d) Ag@RF spheres with 1 mL of ethanol etching at RT for 10 min. Scale bars = 200 nm.

Conclusions

In summary, we report here a dissolution-regrowth process for the preparation of hollow RF nanoparticles with controllable shell thickness. We find that the RF colloidal particles derived by the sol-gel process are heterogeneous in structure, with the near-surface layer being composed of primarily long-chain oligomers and the inside of shorter ones. Such heterogeneity leads to the formation of hollow structures when the particles are subjected to etching by appropriate solvents. Both the condensation degree of the original RF spheres and their etching kinetics are affected by reaction time, temperature, and solvent composition, therefore offering ample opportunities in controlling the morphology of the products from hollow nanoshells to mesoporous structures. Redeposition of the dissolved oligomer to the nanoshells is found to occur at the later stage of the etching process, thus increases the thickness of the nanoshells. We believe this study not only enhances our understanding of the formation and dissolution processes of polymer colloids but also provides a very practical and robust strategy for the preparation of hollow and mesoporous nanostructures without the need of additional sacrificial templates.

Conflicts of interest

There are no conflicts to declare.

Acknowledgements

We are grateful to the financial support from the U.S. National Science Foundation (DMR-1810485). Zhou thanks the China Scholarship Council for supporting his research at UCR.

Notes and references

1. X. He, X. Wu, X. Cai, S. Lin, M. Xie, X. Zhu and D. Yan, *Langmuir*, 2012, **28**, 11929-11938.
2. X. Hu, J. Hu, J. Tian, Z. Ge, G. Zhang, K. Luo and S. Liu, *J. Am. Chem. Soc.*, 2013, **135**, 17617-17629.
3. D. Putnam, *Nat. Mater.*, 2006, **5**, 439.
4. S. R. Guo, J. Y. Gong, P. Jiang, M. Wu, Y. Lu and S. H. Yu, *Adv. Funct. Mater*, 2008, **18**, 872-879.
5. T. Yang, L. Wei, L. Jing, J. Liang, X. Zhang, M. Tang, M. J. Monteiro, Y. Chen, Y. Wang, S. Gu, D. Zhao, H. Yang, J. Liu and G. Q. M. Lu, *Angew. Chem. Int. Ed.*, 2017, **56**, 8459-8463.
6. J. Liu, N. P. Wickramaratne, S. Z. Qiao and M. Jaroniec, *Nature Mater.*, 2015, **14**, 763-774.
7. Y. Nabae, S. Moriya, K. Matsubayashi, S. M. Lyth, M. Malon, L. Wu, N. M. Islam, Y. Koshigoe, S. Kuroki and M.-a. Kakimoto, 2010, **48**, 2613-2624.
8. X. Fang, S. Liu, J. Zang, C. Xu, M.-S. Zheng, Q.-F. Dong, D. Sun and N. Zheng, *Nanoscale*, 2013, **5**, 6908-6916.
9. K. Wang, L. Yang, H. Li and F. Zhang, *Acs Applied Materials & Interfaces*, 2019, **11**, 21815-21821.
10. N. P. Wickramaratne, J. Xu, M. Wang, L. Zhu, L. Dai and M. Jaroniec, *Chem. Mater.*, 2014, **26**, 2820-2828.
11. Y. Shao, L. Zhou, C. Bao and J. Ma, *Carbon*, 2015, **89**, 378-391.
12. Z.-A. Qiao, B. Guo, A. J. Binder, J. Chen, G. M. Veith and S. Dai, *Nano Lett.*, 2012, **13**, 207-212.
13. J. Liu, T. Yang, D.-W. Wang, G. Q. M. Lu, D. Zhao and S. Z. Qiao, *Nat. Commun.*, 2013, **4**, 2798.
14. N. Liu, Z. Lu, J. Zhao, M. T. McDowell, H.-W. Lee, W. Zhao and Y. Cui, *Nature Nanotech.*, 2014, **9**, 187.
15. F. Zhang, X. Liu, M. Yang, X. Cao, X. Huang, Y. Tian, F. Zhang and H. Li, *Nano Energy*, 2020, **69,** 104443.
16. J. Zhu, L. Liao, X. Bian, J. Kong, P. Yang and B. Liu, *Small*, 2012, **8**, 2715-2720.
17. R. Tong and J. Cheng, *Angew. Chem. Int. Ed.*, 2008, **120**, 4908-4912.
18. J. Wang, H. Liu, J. Diao, X. Gu, H. Wang, J. Rong, B. Zong and D. S. Su, *J. Mater. Chem. A*, 2015, **3**, 2305-2313.
19. Y. Wu, Y. Li, L. Qin, F. Yang and D. Wu, *J. Mater. Chem. B*, 2013, **1**, 204-212.
20. Y.-R. Dong, N. Nishiyama, Y. Egashira and K. J. I. Ueyama, *Ind. Eng. Chem. Res.*, 2008, **47**, 4712-4716.
21. J. Liu, S. Z. Qiao, H. Liu, J. Chen, A. Orpe, D. Zhao and G. Q. M. Lu, *Angew. Chem. Int. Ed.*, 2011, **50**, 5947-5951.
22. A. Izumi, T. Nakao and M. Shibayama, *Soft Matter*, 2013, **9**, 4188-4197.
23. S. A. Al‐Muhtaseb and J. A. Ritter, *Adv. Mater*, 2003, **15**, 101-114.

24. K. Z. Gaca and J. Sefcik, *J. Colloid Interface Sci.*, 2013, **406**, 51-59.
25. D.-S. Bin, Z.-X. Chi, Y. Li, K. Zhang, X. Yang, Y.-G. Sun, J.-Y. Piao, A.-M. Cao and L.-J. Wan, *J. Am. Chem. Soc.*, 2017, **139**, 13492-13498.
26. T. Yalcin, Y. Dai and L. Li, *J. Am. Soc. Mass. Spectrom.*, 1998, **9**, 1303-1310.
27. B. Balakrishnan, D. Kumar, Y. Yoshida and A. Jayakrishnan, *Biomaterials*, 2005, **26**, 3495-3502.
28. M. W. Nielen, *Mass Spectrom. Rev.* , 1999, **18**, 309-344.
29. K. Lee, H. Kim, H. Bang, Y. Jung and S. Lee, *Polymer*, 2003, **44**, 4029-4034.
30. W. Stöber, A. Fink and E. Bohn, *J. Colloid Interface Sci.*, 1968, **26**, 62-69.
31. N. T. Thanh, N. Maclean and S. Mahiddine, *Chem. Rev.*, 2014, **114**, 7610-7630.
32. M. I. Vesselinov, *Crystal Growth for Beginners: Fundamentals of Nucleation, Crystal Growth and Epitaxy*, World scientific, 2016.
33. K. Kelton, in *Solid State Physics*, Elsevier, 1991.
34. X. Zhu, S. Wang, W. Huang, Y. Tian and X. Wang, *Carbon*, 2016, **105**, 521-528.
35. S. Zhou, W. Jiang, T. Wang and Y. Lu, *Ind. Eng. Chem. Res.*, 2015, **54**, 5460-5467.
36. M. Zhu and G. Diao, *J. Phys. Chem. C*, 2011, **115**, 18923-18934.
37. J. Zhou, L. Meng, X. Feng, X. Zhang and Q. Lu, *Angew. Chem. Int. Ed.*, 2010, **49**, 8476-8479.
38. Y. Piao, J. Kim, H. B. Na, D. Kim, J. S. Baek, M. K. Ko, J. H. Lee, M. Shokouhimehr and T. Hyeon, *Nat. Mater.*, 2008, **7**, 242.
39. P. Yang, Y. Xu, L. Chen, X. Wang and Q. Zhang, *Langmuir*, 2015, **31**, 11701-11708.

TOC Graphic：